The Effect of Load And Passive Force Component on Muscle Recruitment During Elbow Flexion

Rajnish Kumar[1]
Dr. Sitikantha Roy[1]
Sujash Bhattacharya[1]

Abstract

Information required about the primary human motion to design soft exoskeletons with a human-machine interface for the upper limb, is the measurement of accurate muscle force with and without load. The elbow flexion motion of the upper limb is considered here for determining muscle forces. During elbow flexion, muscles attached across the elbow and shoulder joints create moments. It is a result of very high coordination between our nervous system and the musculoskeletal system. However, not every muscle generates force as most of the human musculoskeletal system is naturally indeterminate. Therefore, one wants to know the pattern of muscle recruitment that our nervous system adopts in normal situations and how it varies during loaded conditions. This study has two objectives: First, to determine how our nervous system recruits specific muscle groups for elbow flexion motion subjected to a load or without it. Secondly, the effect of the passive muscle force component of the on-muscle recruitment and force magnitude. An inverse dynamics approach followed by an optimization has been adopted here. It is found that biceps long head, triceps lateral, and medial head are recruited during no-load motion. In contrast, brachialis and brachioradialis are also recruited during the initial phase of the loaded movement. The effects of the passive component of muscle force are also shown. It was found that as load increases, the recruited muscle force magnitude increases until it reaches the maximum isometric force—further increase in load results in recruitment of new muscles. The result also indicates that the contribution from passive components of muscle cannot be ignored during the elbow flexion motion.

Keywords: *elbow flexion, inverse dynamics, muscle recruitment, loading condition, optimization.*

[1] *Applied mechanics department, Indian Institute of Technology, Delhi*

Introduction

The study, modeling, and simulation of human movement have gained a lot of interest among researchers working in fields of science and industry like biomechanics, medicine, sports science (Lu et al., 2012). Assistive active exo-suits (Lotti et al., 2020), controlled by the human-machine interface, is a very new application field of human musculoskeletal biomechanics, which has revolutionary potential. Design of these exoskeleton devices require models that are the physiologically accurate and fast computation of essential control parameters. The knowledge of multi-body dynamics, muscle-contraction dynamics, and musculoskeletal geometry leads to the quantification of those parameters like joint moments, muscle forces, muscle activations, and excitations. Direct and accurate measurement of these quantities is impossible due to the inability to use invasive methods like surgery while moving the limb. Upper limb motion is prevalent in our day-to-day work and exercises. Elbow flexion is one general motion; however, the coordination needed between our nervous system and the arm musculoskeletal system is complex. For instance, the elbow flexion motion in the sagittal plane can be considered as a result of the rotation of two degrees of freedom, one at the shoulder and another at the elbow joint. There are seven muscles attached across these joints to generate motion. To know which muscles are recruited by our nervous system to develop force in this motion, is an indeterminate problem. Optimization techniques based on a particular criterion have been used extensively to solve these indeterminate problems. Whether linear or nonlinear, all optimization procedures assume that the body selects muscles for a given activity based on some criteria. For instance, an approach that appears to control the muscle load sharing during static posture and motion is the minimization of the weighted sum of all the muscle forces and the forces in the ligaments (Seireg et al., 1975; Hardt 1978). Pedooti et al. (1978) formulated four biologically meaningful optimization criteria and compared the experimental electromyography (EMG) data with the muscle force patterns obtained computationally under the various performance criteria. For the first time, Kaufman et al. (1991) used the minimization of neuromuscular activation to know muscle contraction during a motion. In the present work, the objective function minimized to find muscle forces, is the sum of activation squared (Anderson et al., 2001). Muscle activations are the parameter which represents the pattern of muscle recruitment by the human nervous system. In literature, muscle activations and neural excitations are widely used parameters to quantify muscles' neural control. These two parameters can also be related using 'First order activation dynamics' (Zajac et al. 1989, Winters et al. 1995) or 'Second-order nonlinear activation dynamics' (Buchanan et al., 2005). Manal et al. (2003) showed how muscle activation and excitation are related to electromyogram (EMG) signals.

In this study, a two-link and seven muscle model of the upper limb has been considered. Joint moments generated during elbow flexion motion has been computed using the equation of motion derived for this model. As mentioned earlier, static optimization with an optimal criterion is adopted to calculate forces and activations of the muscle groups. The effects of loading conditions on the muscle forces are depicted in the results. The effect of including the passive component in total muscle force is also investigated and discussed.

Problem Formulation

The human upper limb has 7 degrees of freedom (DOF) without considering hand DOFs; elbow flexion motion in the sagittal plane involves two DOFs, one at the shoulder joint and the other at the elbow, both assumed as revolute joints (London, 1981 and Holzbaur et. al., 2005). The two segments involved in motion are the upper arm (humerus) and the lower arm (ulna and radius are considered as a rigid segment). Major force-generating agonist muscles in this motion are biceps short head, biceps long head, brachialis, and brachioradialis. In contrast, the antagonist muscles involved are triceps long head, triceps lateral head, and triceps medial head.

Therefore, we are assuming that these seven muscles are responsible for the elbow flexion motion. All muscles are modeled as modified Hill-type, as described by Thelen (2003). Tendons are assumed as rigid and only transferring the muscle force to the bones through attachment points. This whole upper limb has been modeled as a stick model (Figure 1) where humerus is considered one link and ulna and radius as other links with equivalent segment length, mass, mass moment of inertia, and center of mass location. M_1 and M_2 are the moments at the shoulder and elbow joint generated by the muscle forces attached across. The moment arm is the perpendicular distance of the line of action of muscle forces to the center of each joint rotation during elbow flexion. As the line of action of muscle force changes with the joint's angle of rotation, the moment arm also changes. The muscle fiber length varies with the elbow flexion motion. The polynomial equations generated by Pigeon et al. (1996) for the moment arm's variation and muscle length variation with the joint angle has been used to compute the muscle length change during elbow flexion. Mono articular muscle length is a function of a single joint angle across which they are attached, whereas bi-articular muscle passes two joints, so their lengths are functions of two joint angles that they run across. Here brachialis and brachioradialis are mono-articular, and biceps brachii and triceps brachii are bi-articular muscles.

Solution Methodology

Once the model has been developed, to know muscle activation pattern by solving an inverse dynamics problem following steps has been followed:

The multi-body equation of motion is formulated for the equivalent stick model using Lagrange's equation of the second kind. Using inertial properties, velocity, and acceleration, the equation of motion is solved to get joint moments. Movement trajectory data is collected, and angular velocity and acceleration of the upper and lower arm are computed. These are the input to the derived equations of motion to compute moments at both joints. An optimization problem is solved considering the physiology of muscles to find recruitment and activations of muscles. Further, the changes in the recruitment pattern are studied while the arm is subjected to load.

Step 1: The human upper limb consists of two segments, i.e., upper arm and forearm with hand. The model was converted into an equivalent stick model by considering the whole upper arm with bones and muscles considered as one link, similarly entire forearm with bones and muscles as another link. In this study, both shoulder and elbow joints are assumed as a simple hinge with a single degree of freedom. For elbow flexion, force-generating muscle groups are biceps brachii, brachialis, brachioradialis, and triceps brachii. The necessary parameters, such as the moment of inertia (MOI), location of the center of mass (Table 1) of segments is taken according to the investigation performed by Challis and Kerwin (1992). According to Challis and Kerwin (1992), the percentage error in the MOI calculation by Hinrichs (1985) technique is minimum. A set of regression equations developed by Hinrichs (1985) has been applied to compute Moment of Inertia (MOI) about the transverse axis (normal to sagittal plane) passing through each segment's center of mass using the data of Chandler et al. (AMRL Technical Report 74- 137).

Figure 1: Equivalent stick model of the upper limb in the sagittal plane

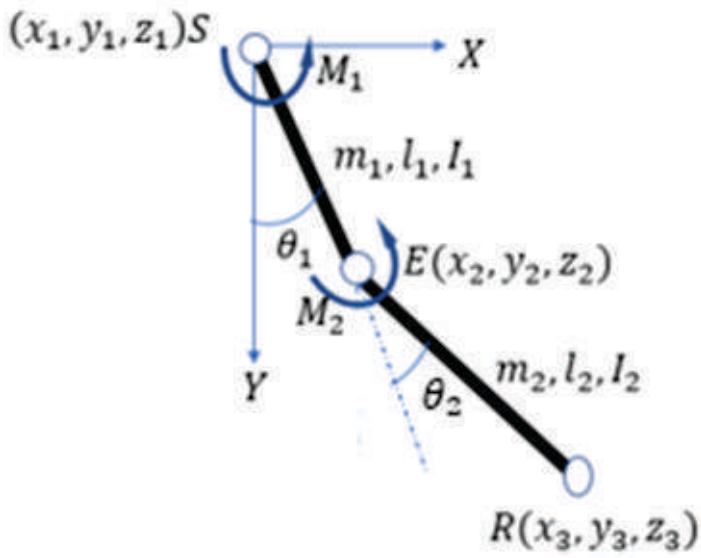

Figure 2: Flow chart of the method to solve an inverse problem

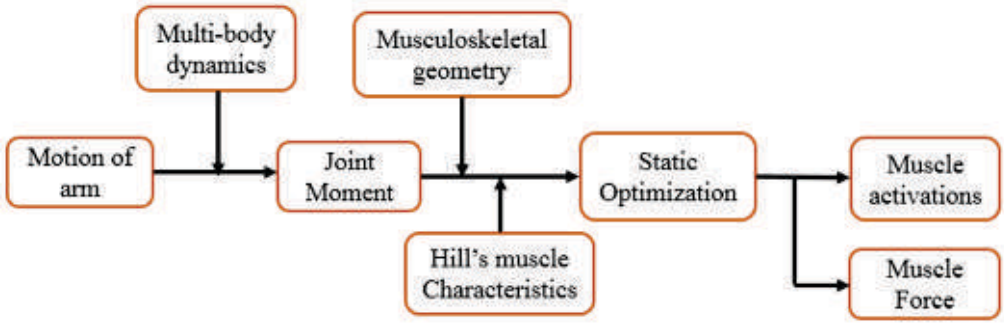

Table 1 : Location of Centre of mass: (X_1, Y_1) and (X_2, Y_2) are the center of mass of the upper and lower arm, respectively

Segment	Centre of mass (COM)
Upper arm	$X_1 = 0.449 l_1 \sin\theta_1 \qquad Y_1 = 0.449 l_1 cos\theta_1$
Lower arm with the hand	$X_2 = l_1 sin\theta_1 + 0.382 l_2 \sin(\theta_1 + \theta_2)$ $Y_2 = l_1 cos\theta_1 + 0.382 l_2 \cos(\theta_1 + \theta_2)$

Step 2: Multi-body dynamic equation of motion with external load for the equivalent two link stick model is derived using Lagrange's equation

$$\begin{bmatrix} M_1 \\ M_2 \end{bmatrix} = \begin{bmatrix} (I_1 + 0.2016m_1l_1^2 + I_2' + m_2'l_1^2) & (I_2' + Pl_1l_2\cos(\theta_1 - \theta_2)) \\ (I_2' + Pl_1l_2\cos(\theta_1 - \theta_2)) & (I_2' + P^2m_2'l_2^2) \end{bmatrix} \begin{Bmatrix} \ddot{\theta}_1 \\ \ddot{\theta}_2 \end{Bmatrix} + \begin{bmatrix} Pl_1l_2\,sin(\theta_1 - \theta_2) & 0 \\ 0 & -Pl_1l_2\,sin(\theta_1 - \theta_2) \end{bmatrix} \begin{Bmatrix} \dot{\theta}_2^{\,2} & 0 \\ 0 & \dot{\theta}_1^{\,2} \end{Bmatrix} + \begin{bmatrix} -(0.449m_1gl_1 + m_2'gl_1)\,sin\,\theta_1 \\ -Pm_2'gl_2\,sin\,\theta_2 \end{bmatrix} \quad (1)$$

Where

$$I_2' = I_2 + m_2\big((P - 0.382)l_2\big)^2 + m\big((0.618 - P)l_2\big)^2$$
$$m_2' = m_2 + m$$
$$P = \frac{0.382m_2 + m}{m_2 + m}$$

In equation (1) M_1, M_2 are the moments at the shoulder and elbow joints, respectively. I_1, I_2 are the moments of inertia of the upper and lower arm about an axis passing through the center of mass normal to the sagittal plane. m_1, m_2 & l_1, l_2 are the mass and length of the upper and lower arm, respectively. m is the external load on the lower arm. θ_1, θ_2 are the angular position of the upper and lower arm, respectively.

Step 3: In this step, the variation of joint angles with time is computed using the motion capture data for the whole arm's trajectory during elbow flexion available in the literature (arm26_inversekinematics. mot file available in OpenSim), at a rate of 120 Hz. The relevant motion data used here was acquired through an optical motion capture system and reflective markers following the International Society of Biomechanics (ISB) recommendations on anatomical locations and marker positions. For right arm motion in the sagittal plane, the markers are Acromion, Humerus epicondyle, and Radius styloid. Using the angular variation of segments at each time step, we computed angular velocity and angular acceleration for both upper and lower arm using first-order and second-order Taylor series approximation, respectively. These kinematic data as input and the equation of motion derived in the previous step along with the inertial properties; we computed the moment required at each joint in MATLAB.

Step 4: Now, to know which muscles are recruited and the magnitude of force developed in them, an optimization problem has been solved at each time step of the motion trajectory. The formulation of physiological static optimization is as follows: The objective function to be minimized is the sum of all the muscles activation squared $J = \sum_{i=1}^{n}(a_i(t_k))^2$ (Anderson et al., 2001), subjected to constraints $R_{ji}(\theta(t_k))F_i^M(t_k) = M_j(t_k)$ And $0 \le a_i(t_k) \le 1$. Here, $a_i(t_k)$ is the activation of the i^{th} muscle at k^{th} time instant, $F_i^M(t_k)$ is the muscle force generated in the muscle at the k^{th} time instant, $R_{ji}(\theta(t_k))$ is the i^{th} muscle moment arm at j^{th} j joint as a function of the joint angle at k^{th} time instant, $M_j(t_k)$ is the moment at j^{th} joint at k^{th} time instant. The activation of the i^{th} muscle at k^{th} time instant is defined as $a_i(t_k) = \frac{F_i^M(t_k)}{f(F_i^o, l_m, v_m)}$ where $F_i^M(t_k)$ is the muscle function $f(F_i^o, l_m, v_m)$ is the muscle force generated. The is the force-length-velocity relationship (Anderson et al., 2001), for the i^{th} muscle, where F_i^o is the

maximum isometric force and l_m is the muscle fiber length, v_m is the rate of change of the muscle fiber length. Here, it is assumed that humans put effort to generate only active muscle force, which is given as $F_i^M(t_k) = a_i(t_k)f(F_i^o, l_m, v_m)$. The range of activation a is between 0 and 1 means when a = 0 muscle is no activated at all and generating no force and when a = 1 muscle is fully activated and generating maximum force. This physiological static optimization has been solved using the MATLAB function "fmincon" for activations and muscle forces. The result and discussion are presented in the following section.

Result and Discussion

The muscle recruitment pattern and effect of passive components results are shown for the variation in elbow flexion angle and shoulder angle for the trajectory given in Figure 3. In step 4, the moments computed for the trajectory are shown in (Figure 4) is similar to inverse dynamics result from OpenSim (Delp et al., 2007 and Seth et al., 2018) for arm26 model using the same trajectory (Figure 3). However, there is a slight difference in the shoulder moment result after 0.5 seconds. One of the reasons for this variation could be little difference in the inertial parameters such as segmental mass, the moment of inertia, the center of mass location. Here, the shoulder joint is considered as fixed to the ground. The moment generated at this joint is $M_1 + M_2$ It also provides a counter moment to make the shoulder joint remain stable due to the moment generated at the elbow joint.

Figure 3: The trajectory of the shoulder and elbow joint angle with time

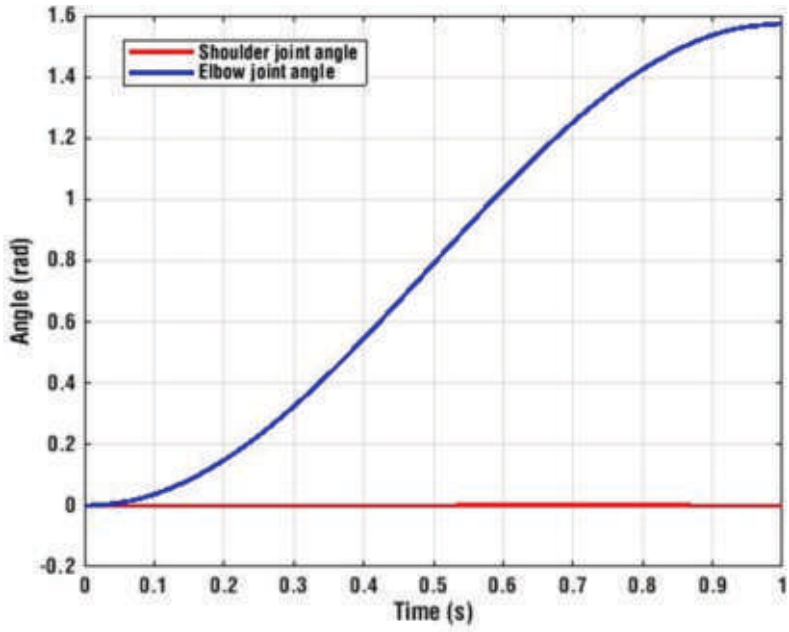

The force predicted in the muscles (Figure 5) in the present work (dashed lines) is similar to the result of static optimization from OpenSim (Solid lines). The magnitude of maximum and average muscle force generated for the no-load condition is given in Table 2. In the present study, six muscles have been considered biceps short head, biceps long head, brachialis, triceps long head, triceps lateral head, and triceps medial head as the arm26 model OpenSim also has six muscle. In this result, the passive component of muscle, as described in Thelen (2003), has not been considered in the simulation.

Figure 4: Joint moments validation plot of the present study (dashed lines) with OpenSim (solid lines)

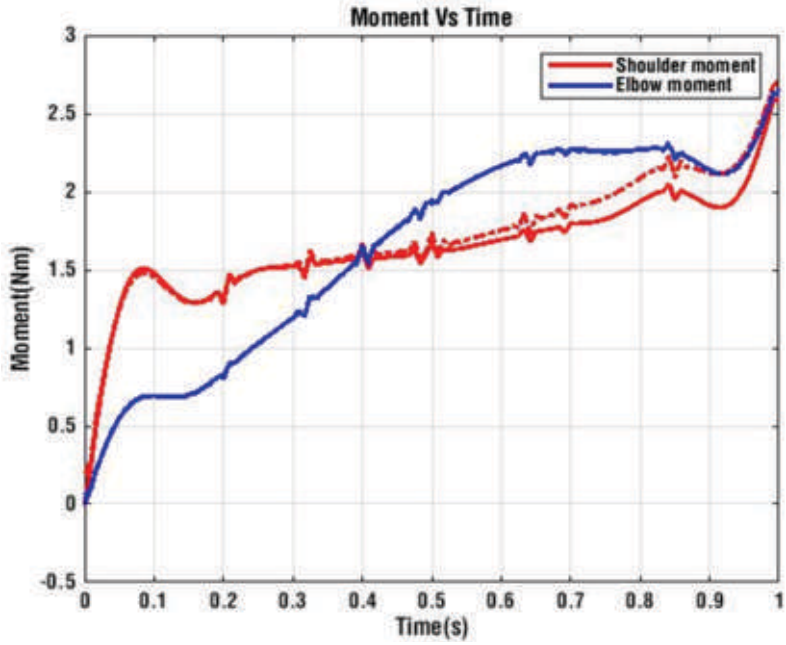

Figure 5: Muscle recruitment validation plot of present work (dashed lines) and OpenSim (solid lines)

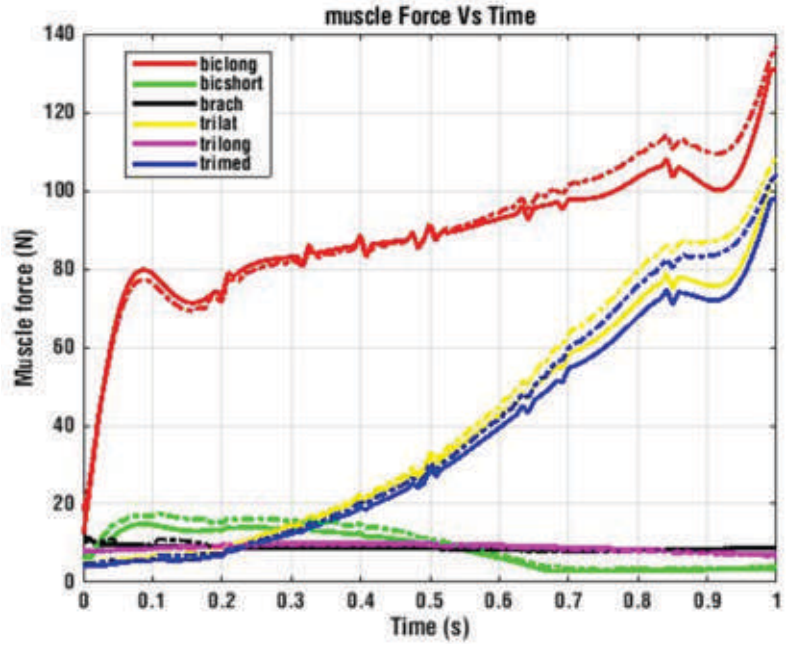

Our second objective was to determine the effect of adding passive muscle force to muscle recruitment and muscle force magnitude. We added a passive muscle component in our existing model and compared for the same trajectory to visualize the impact. Figure 6 shows muscle recruitment and force magnitude changes when the passive component force is also included in the model. The result indicates that along with biceps long head, triceps lateral head, triceps medial head, one more muscle triceps long head (Figure 6, purple dashed line) also contributes. Table 2 indicates the magnitude of maximum and average muscle force during all loading conditions.

Figure 6: Muscle force after including a passive component of the muscle to the model (dashed lines) and muscle force without passive component (solid lines).

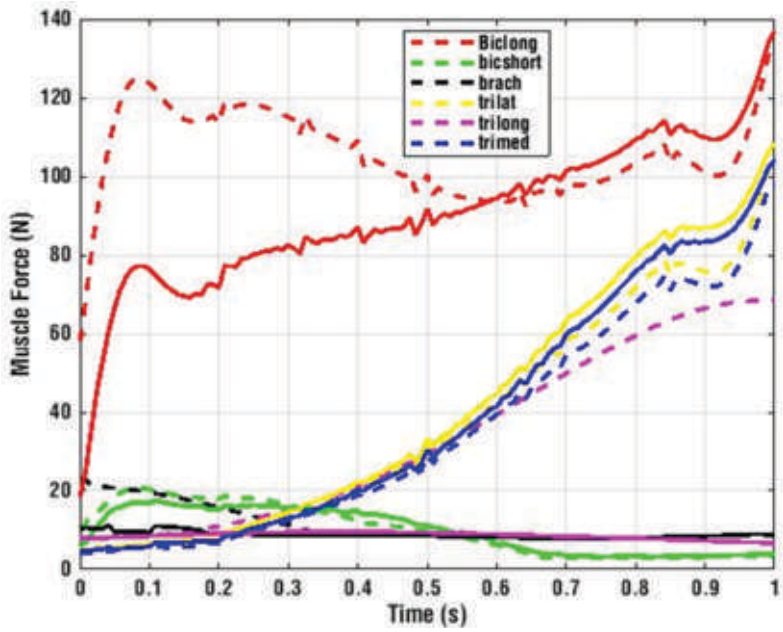

The magnitude of biceps long head (Figure 6) muscle force increased by the passive component's value until the motion's 0.5 sec duration. This increase has resulted because, during this movement interval, biceps long head muscle length was more than its optimum length. That is, it was already in a lengthened condition at the beginning of the motion. According to Hill's force-length characteristic curve (Thelen 2003), passive force becomes evident during the muscle's lengthening. After 0.5 sec, there is a small decrease in the biceps long head muscle force for the rest of the motion.

The result (Figure 6) also shows a little decrease in lateral triceps head (trilat) and triceps medial head (trimed) force. This decrease is due to the passive element present in the muscle assisting the contractile component in the overall antagonistic muscle action during the motion. The activation of triceps long head (trilong) muscle is due to that the muscle length is more than optimum muscle length during the movement.

To study the effect of load on the muscle recruitment, we added brachioradialis (brd) muscle in our model to visualize the impact during this elbow flexion motion. The predicted result for 2kg and 3kg of the load is shown in Figures 7(a) and 7(b), respectively, showing that brachialis (brach) is also activated for the movement duration of 0.2 sec. Figure 8(a) and 8(b) shows muscle recruitment for a 5kg and 8kg load

respectively in hand; all seven muscles are activated along with brachioradialis. It is clear that muscles are recruited and activated as per requirement against the hand's load. For an 8kg load, all seven muscles are activated with an increased magnitude of muscle forces. The muscle recruitment pattern and magnitude of forces shown in Figures 7 and 8 include both the active and passive force of the muscle.

Muscle recruitment patterns during the relevant motion can be analyzed by calculating muscle activations, as mentioned in the introduction. Figure 9(a) and 9(b) represents the muscle activations during no-load condition and for 5 kg load. The plots show that with an increase in load, muscle recruitment pattern changes significantly. In the case of 5 kg load, the muscles like bicep long and short attain their maximum activation, thus failing to generate more force. Hence, the neural control system activates other muscles like brachialis.

Table 2: The average and maximum force (N) generated in the muscles

Muscles	No-Load		2Kg		3Kg		5Kg		8Kg	
	Avg	Max	Avg	Max	Avg	Max	Avg	Max	Avg	Max
Biceps Long head (biclong)	105.64	130.94	355.90	527.60	449.45	573.18	487.00	594.74	491.91	597.51
Biceps short head (bicshort)	9.95	20.52	34.56	74.10	135.38	280.64	303.81	427.68	330.28	431.03
Brachialis (brach)	11.21	21.46	21.10	92.15	27.76	140.58	89.92	262.85	111.09	287.44
Brachioradialis (brd)	5.50	11.69	5.69	13.46	6.04	16.19	27.91	63.60	33.85	65.11
Triceps lateral head (trilat)	39.28	105.65	127.09	379.77	216.36	615.29	301.97	624.94	288.78	577.25
Triceps long head (trilong)	33.93	68.60	33.93	68.60	33.93	68.60	33.93	68.60	33.93	68.60
Triceps medial head (trimed)	36.62	100.67	118.82	361.80	201.98	601.10	284.13	610.41	272.19	557.71

Figure 7(a): Muscle recruitment and total muscle force for 2 Kg load

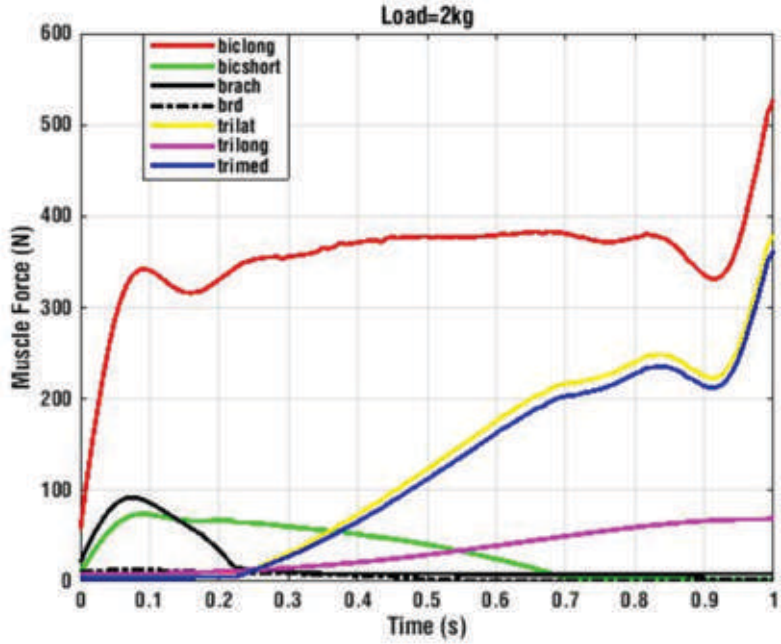

Figure 7(b): Muscle recruitment and total muscle force for 3kg load

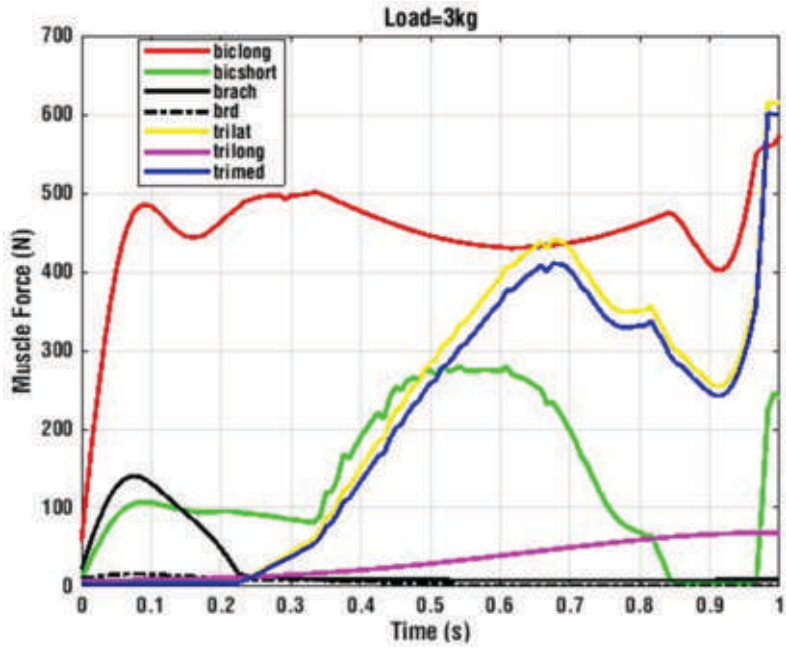

Figure 8(a): Muscle recruitment and total muscle force for 5 Kg load

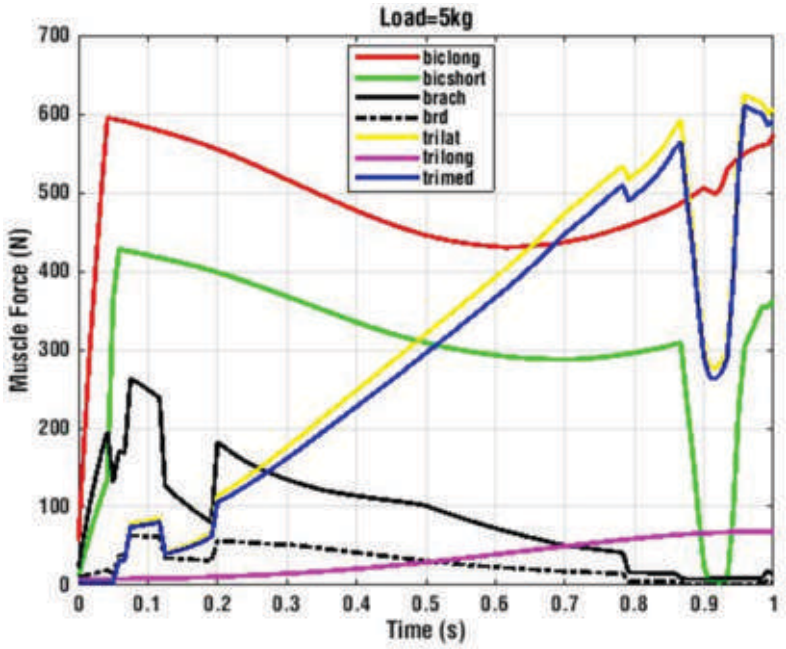

Figure 8(b): Muscle recruitment and total muscle force for 8kg load

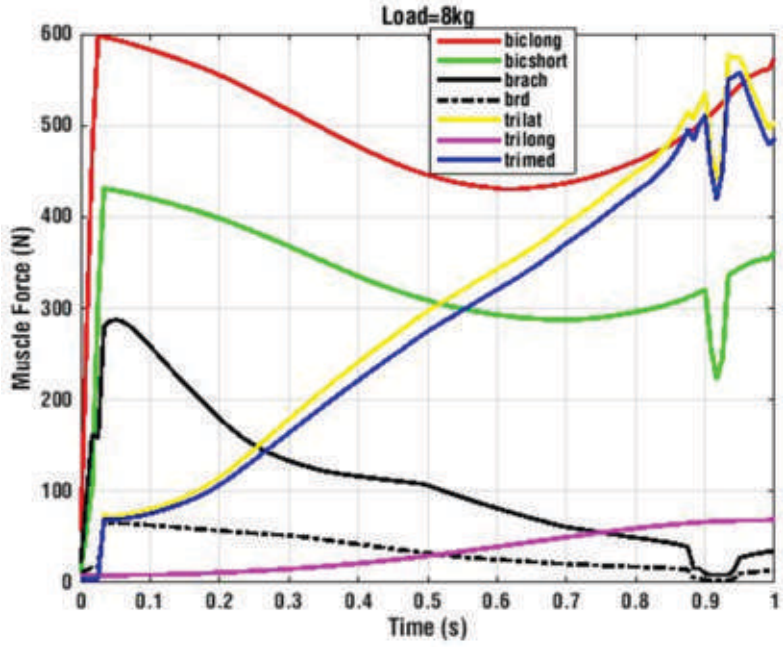

Figure 9(a): Muscle activations for no load condition

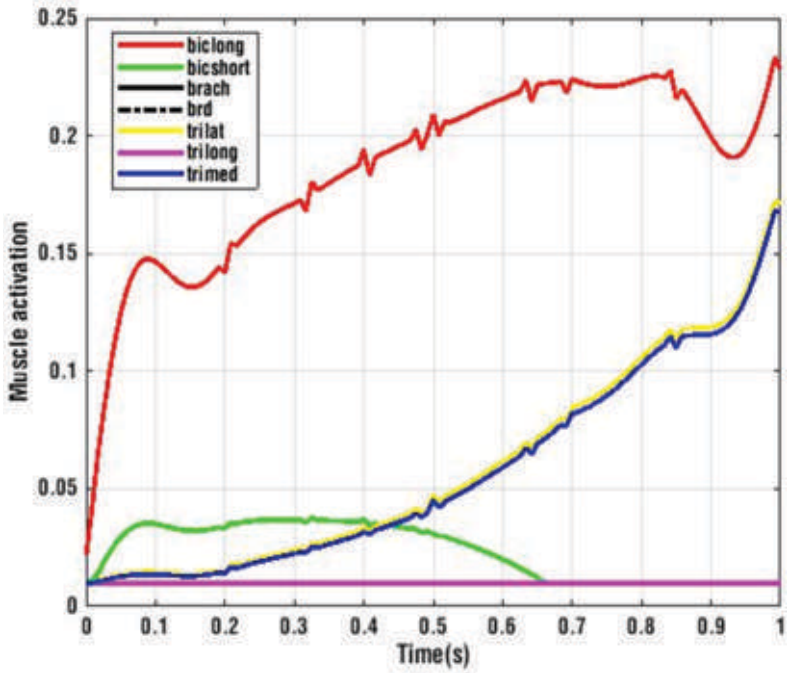

and brachioradialis and generate significant force. This phenomenon is also reflected in Figure 8(a), where a significant increase in these muscles' forces can be observed.

Figure 9(b): Muscle activations for 5 kg load

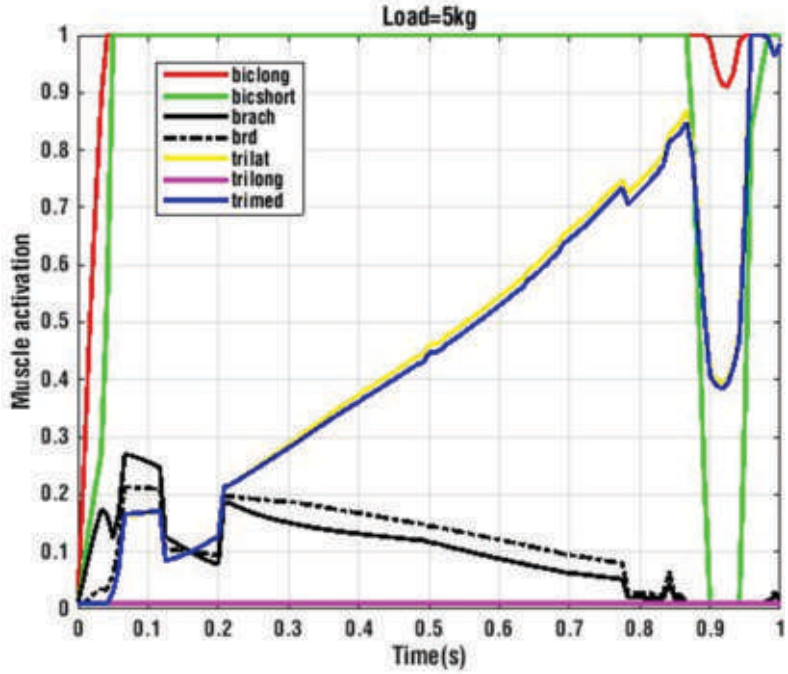

Conclusion

This study establishes the effect of load on the muscle recruitment pattern while doing elbow flexion. It is found that Biceps long head, Triceps lateral, and medial head are recruited during no-load motion. In contrast, brachialis and brachioradialis are also recruited during the initial phase of the loaded movement. The effects of the passive component of muscle force are also shown. It was found that as load increases, the recruited muscle force magnitude increases until it reaches the maximum isometric force—further increase in load results in recruitment of new muscles. Result also indicates that the contribution from passive components of muscle cannot be ignored during the elbow flexion motion.

References

- Alexander, R. (1995). Simple models of human movement. *Applied Mechanics Reviews*, *48*(8), 461-470.
- Anderson, F. C., & Pandy, M. G. (2001). Static and dynamic optimization solutions for gait are practically equivalent. *Journal of biomechanics*, *34*(2), 153-161.
- Arvikar, R. J., & Seireg, A. (1975). The prediction of muscular load sharing and joint forces in the lower extremities during walking. *Journal of biomechanics*, *8*(2), 89-102.
- Buchanan, T. S., Lloyd, D. G., Manal, K., & Besier, T. F. (2004). Neuromusculoskeletal modeling: estimation of muscle forces and joint moments and movements from measurements of neural command. *Journal of applied biomechanics*, *20*(4), 367-395.
- Challis, J. H., & Kerwin, D. G. (1992). Calculating upper limb inertial parameters. *Journal of sports sciences*, *10*(3), 275-284.
- Crowninshield, R. D. (1978). Use of optimization techniques to predict muscle forces.
- Crowninshield, R. D., & Brand, R. A. (1981). A physiologically based criterion of muscle force prediction in locomotion. *Journal of biomechanics*, *14*(11), 793-801.
- Delp, S. L., Anderson, F. C., Arnold, A. S., Loan, P., Habib, A., John, C. T., Guendelman, E. & Thelen, D. G. (2007). OpenSim: open-source software to create and analyze dynamic simulations of movement. *IEEE transactions on biomedical engineering*, *54*(11), 1940-1950.
- Garner, B. A., & Pandy, M. G. (2001). Musculoskeletal model of the upper limb based on the visible human male dataset. *Computer methods in biomechanics and biomedical engineering*, *4*(2), 93-126.
- Gordon, C. C., Churchill, T., Clauser, C. E., Bradtmiller, B., McConville, J. T., Tebbetts, I. & Walker, R. A. (1989). Anthropometric survey of U.S. Army personnel:Summarystatistics, interim report for 1988.
- Hardt, D. E. (1978). Determining muscle forces in the leg during normal human walking an application and evaluation of optimization methods.
- Hinrichs, R. N. (1985). Regression equations to predict segmental moments of inertia from anthropometric measurements: an extension of the data of Chandler et al. (1975). *Journal of Biomechanics*, *18*(8), 621-624.
- Holzbaur, K. R., Murray, W. M., & Delp, S. L. (2005). A model of the upper extremity for simulating musculoskeletal surgery and analyzing neuromuscular control. *Annals of biomedical engineering*, *33*(6), 829-840.
- Kaufman, K. R., An, K. N., Litchy, W. J., & Chao, E. Y. S. (1991). Physiological prediction of muscle forces - I. Theoretical formulation. *Neuroscience*, *40*(3), 781- 792.
- Krishnan, R. H., Devanandh, V., Brahma, A. K., & Pugazhenthi, S. (2016). Estimation of mass moment of inertia of human body, when bending forward, for the design of a self-transfer robotic facility. *Journal of Engineering Science and Technology*, *11*(5), 166-76.
- London, J. T. (1981). Kinematics of the elbow. *JBJS*, *63*(4), 529-535.
- Lotti, N., Xiloyannis, M., Durandau, G., Galofaro, E., Sanguineti, V., Masia, L., & Sartori, M. (2020). Adaptive model-based myoelectric control for a soft wearable arm exosuit: A new generation of wearable robot control. *IEEE Robotics & Automation Magazine*, *27*(1), 43-53.

- Lu, T. W., & Chang, C. F. (2012). Biomechanics of human movement and its clinical applications. *The Kaohsiung journal of medical sciences*, *28*, S13-S25.
- Manal, K., & Buchanan, T. S. (2003). A one-parameter neural activation to muscle activation model: estimating isometric joint moments from electromyograms. *Journal of biomechanics*, *36*(8), 1197-1202.
- Maurel, W., Thalmann, D., Hoffmeyer, P., Beylot, P., Gingins, P., Kalra, P., & Thalmann, N. M. (1996). A biomechanical musculoskeletal model of the human upper limb for dynamic simulation. *Computer Animation and Simulation* (121-136).
- Pandy, M. G. (2001). Computer modeling and simulation of human movement. *Annual review of biomedical engineering*, *3*(1), 245-273.
- Patriarco, A. G., Mann, R. W., Simon, S. R., & Mansour, J. M. (1981). An evaluation of the approaches of optimization models in the prediction of muscle forces during human gait. *Journal of Biomechanics*, *14*(8), 513-525.
- Pedotti, A., Krishnan, V. V., & Stark, L. (1978). Optimization of muscle-force sequencing in human locomotion. *Mathematical Biosciences*, *38*(1-2), 57-76.
- Pigeon, P., & Feldman, A. G. (1996). Moment arms and lengths of human upper limb muscles as functions of joint angles. *Journal of biomechanics*, *29*(10), 1365-1370.
- Pontonnier, C., & Dumont, G. (2009). Inverse dynamics method using optimization techniques for the estimation of muscle forces involved in the elbow motion. *International Journal on Interactive Design and Manufacturing (IJIDeM)*, *3* (4), 227.
- Rahikainen, A. (2015). Modeling muscle mechanics of arm and leg movement: a new approach to Hill's equation. *Studies in sport, physical education, and health*, (227).
- Seth, A., Hicks, J. L., Uchida, T. K., Habib, A., Dembia, C. L., Dunne, J. J., Ong, C. F., DeMers, M. S., Rajagopal, A., Millard, M. & Hamner, S. R. (2018). OpenSim: Simulating musculoskeletal dynamics and neuromuscular control to study human and animal movement. *PLoS computational biology*, *14*(7), 1006223.
- Thelen, D. G. (2003). Adjustment of muscle mechanics model parameters to simulate dynamic contractions in older adults. *J. Biomech. Eng.*, *125*(1), 70-77.
- Winters, J. M. (1995). An improved muscle-reflex actuator for use in large-scale neuromusculoskeletal models. *Annals of biomedical engineering*, *23*(4), 359-374.
- Zajac, F. E. (1989). Muscle and tendon: properties, models, scaling, and application to biomechanics and motor control. *Critical reviews in biomedical engineering*, *17*(4), 359-411.

Rajnish Kumar *is a Research Scholar, Department of Applied Mechanics, Indian Institute of Technology Delhi, New Delhi 110016. He can be reached at rajnish.kuram92@gmail.com*

Sitikantha Roy *is Associate Professor, Department of Applied Mechanics, Indian Institute of Technology-Delhi, New Delhi 110016. He can be reached at sitiroy@gmail.com*

Sujash Bhattacharya *is a Research Scholar, Department of Applied Mechanics, Indian Institute of Technology Delhi, New Delhi 110016. He can be reached at iamsujash@gmail.com*

The effects of Alpha/Theta neurofeedback due to Shirodhara Treatment

Yogeshwar Dasari[1]
Swathika M[2]
Anita Teladevalapalli[3]
Lakshmana Rao Chebolu[1]
Venkatesh Balasubramanian[4]

Abstract

Shirodhara is a traditional ayurvedic method of healing in which medicated liquid is poured on the human forehead and it has been in use since ancient times to bring the mind, body, and soul to a harmonious level. The effectiveness of Shirodhara treatment can be measured by EEG. Various liquids can be used such as medicinal oils, water, buttermilk, but the present study uses medicinal oil named "Ksheerabala thailam". This treatment results in the relaxation of the brain and to some extent the onset of drowsiness. To show the effectiveness of Shirodhara treatment, Alpha/Theta ratio neurofeedback has been calculated, as Alpha/Theta is an indicator between relaxation and sleep. Apart from this, alpha waves have also been analyzed as alpha waves are found in a state of wakeful rest. The median frequencies of each band alpha, as well as theta band, has been analyzed to know in which range the EEG waves are produced and state whether the person is in a relaxed or lethargic state post-Shirodhara treatment.

Keywords: *Shirodhara, EEG, Alpha, Theta, Relaxation, Median frequency.*

[1] *Department of Applied Mechanics, IIT Madras, Chennai*
[2] *Modelling and Simulation Engineer, Schlumberger Ltd, Coimbatore*
[3] *Department of Information Technology, Velagapudi Ramakrishna Siddhartha Engineering College, Vijayawada*
[4] *Department of Engineering Design, IIT Madras, Chennai*